2013 IEEE/RSJ International Conference on
Intelligent Robots and Systems (IROS)
November 3-7, 2013. Tokyo, Japan

Natural Local Approximation based Contouring Control for Free-form Contours

Hao Meng, Yunjiang Lou and Jiangpeng Zhou

Abstract— **In this paper, a novel contouring control method based on natural local approximation of desired contour in task frame is proposed for multi-axis control systems. Based on local geometry properties, natural local approximation can achieve more accurate contouring error estimation compared with other local approximation methods for both planar and spatial contouring tasks. The contouring controller, integrated with a PD controller cooperated with the feedback linearization technique and a feedforward compensation, is designed to realize the decoupling control of estimated errors in the task frame. Contouring performance can then be improved directly by increasing corresponding controller parameters. Simulations of 3-axis system and experiments on biaxial XY-stage verified that our proposed method can reduce the contouring errors dramatically in high speed and large curvature cases compared with first-order based method.**

I. Introduction

Contouring control is crucial to improve the surface quality of machined parts in high-speed and high-precision manufacturing. However, contouring error is not always consistent with the tracking one. As illustrated in Fig. 1, smaller tracking error may lead to larger contouring error by comparing actual points A_1 and A_2. Therefore, contouring error is more important in precision contouring control.

Koren [1] proposed the Cross-Coupled Controller (CCC) aimed at making the contouring error control closed-loop. Feedback corrective actions of real-time computed contouring error are added to existing individual controllers to strengthen the contouring system coordination. Many researches have developed this method by improving the contouring error estimation accuracy [2][3] or proposing more effective contouring controllers [4][5][6].

To directly control the contouring error dynamics, another approach tackled the contouring control problem in task frames. Chiu and Tomizuka [7] proposed a local task coordinate frame (TCF) approach. In the task frame attached to the desired contour, the normal part of the tracking error is treated as the estimated contouring error and they achieved decoupling control of the error dynamics in the tangential and normal directions. The moving TCF based contouring control approach has been applied in [8][9][10][11].

Since the contouring error is the shortest distance from the current actual position to the desired contour, its real-time computation is complicated and difficult for general freeform contours [12]. The contouring error estimations utilized by most of above-mentioned researches can be categorized as the local approximations, including the tangent line and the circular approximation, as the desired contour is locally replaced by the tangent line or osculating circle attached to it in the contouring error estimation. The tangent line approximation, which is actually the first-order Taylor expansion at the desired position, can achieve accurate contouring error estimation for small-curvature and/or small-torsion contours. But the estimation accuracy deteriorates in high-speed and large-curvature cases. To overcome this defect, Yang and Li [13] recently proposed the circular approximation, a second-order approximation method. However, this method is limited to 2-dimension planar or small torsion 3-dimension spatial contours.

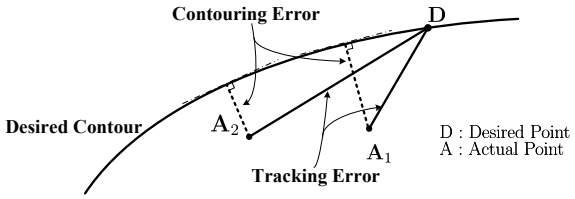

Fig. 1. Tracking error and contouring error

For the desired contour described by algebraic equations, Chen and Wu [14] took the equivalent error as an estimation of the contouring error and Yao's group [15][16] recently proposed the orthogonal global task coordinate frame (GTCF). The above contouring error estimation methods depend only on desired contour's geometric properties and are time-independent as well. However, it is still not easy to find the algebraic equation for any freeform contours.

In this paper, we propose a novel contouring control method based on natural local approximation of desired contour for multi-axis systems. This paper is organized as follows. In section II, contouring error estimation based on natural local approximation of desired contour is briefly introduced. In section III, system dynamics in the fixed world frame is transformed into the task frame. Decoupled controller is designed to assign different dynamics in the task frame with an emphasize on minimizing the contouring errors. In section IV, simulations of 3-axis system and experiments on biaxial XY-stage are conducted to compare this proposed method with first-order based one. Conclusions are given in section V.

This work was supported by the National Natural Science Foundation of China (No. 51075085) and the Key Joint Project of National Natural Science Foundation of China (No. U1134004).

Hao Meng, Yunjiang Lou and Jiangpeng Zhou are with the School of Mechanical Engineering and Automation, Harbin Institute of Technology Shenzhen Graduate School and Shenzhen Key Lab for Advanced Motion Control and Modern Automation Equipments, Shenzhen, China. (Email: hit.meng.h@gmail.com, louyj@hitsz.edu.cn, hit.zhou.jp@gmail.com)

II. Local estimation of contouring error

In this section, the local Frenet frame attached to the desired contour and the canonical form are briefly introduced and discussed at first. Then, a local approximate curve is proposed to estimate the contouring error.

A. Local Frenet Frame

Let smooth curve $c_d(t): I \to \mathbb{R}^3$ be the desired contour in the 3-dimension space, where the generalized coordinate t is regarded as the time in this paper for convenience. For the study of curve, $c_d(t)$ is assumed to be regular and 3-orders continuous differential at least.

In the world Cartesian coordinate frame $\mathscr{F}_w$, the parametric equation of $c_d(t)$ is given by

$$c_d(t) := w_d(t) = \begin{bmatrix} \mathrm{x_d}(t) \\ \mathrm{y_d}(t) \\ \mathrm{z_d}(t) \end{bmatrix} \tag{1}$$

For any point on the desired curve, there exists an exclusive 3-dimension Frenet frame $\mathscr{F}_f$ attached to it with α,β and γ being its orthogonal basis [17].

$$\begin{aligned} \alpha &= \frac{\dot{w}_d}{\|\dot{w}_d\|} \\ \beta &= \gamma \times \alpha \\ \gamma &= \frac{\dot{w}_d \times \ddot{w}_d}{\|\dot{w}_d \times \ddot{w}_d\|} \end{aligned}$$

where $\dot{w}_d = \frac{dw_d}{dt}$ and $\ddot{w}_d = \frac{d^2 w_d}{dt^2}$, and $\|\cdot\|$ represents 2-norm of vectors. Also note that the parameter t is omitted for brevity. Unit vectors α, β and γ represent the tangential, normal and binormal directions respectively.

Let $f = [\mathrm{t}, \mathrm{n}, \mathrm{b}]^T$ be the coordinates of Frenet frame. The transformations between $\mathscr{F}_w$ and $\mathscr{F}_f$ are

$$T_{fw} : w = Rf + w_d \tag{2}$$

$$T_{wf} : f = R^{-1}(w - w_d) \tag{3}$$

where $R = [\alpha, \beta, \gamma]$ and $R^{-1} = R^T$. The calculations of curvature κ and torsion τ are listed below

$$\kappa = \frac{\|\dot{w}_d \times \ddot{w}_d\|}{\|\dot{w}_d\|^3} \tag{4}$$

$$\tau = \frac{(\dot{w}_d, \ddot{w}_d, \dddot{w}_d)}{\|\dot{w}_d \times \ddot{w}_d\|^2} \tag{5}$$

where $(\cdot,\cdot,\cdot)$ represents the mixed product. In the light of (4) and (5), the curvature is always positive, while the torsion is not, which can also be seen in Fig. 2.

The Frenet frame has been utilized in the contouring control study. However, previous researches locally approximate the desired contour as the tangent line, a first-order approximation. And the normal error is treated as the estimated contouring error, which is not effective in the case of high speed and large curvature manufacturing. In the following, the canonical form of desired regular curve at a point is introduced in brief and higher-order approximation is applied in contouring error estimation.

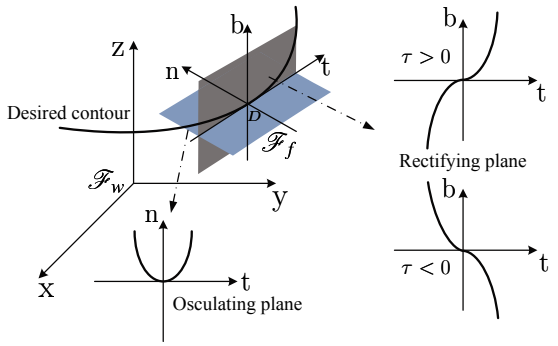

Fig. 2. Local Frenet frame and canonical form of desired contour

B. Local Canonical Form

To investigate the local geometric properties of desired contour, the following introduction and discussion are carried out in the Frenet Frame. The above regular curve c_d is re-parameterized by the arc length s, and the origin of the Frenet frame, the desired point D on the desired contour in Fig.2, is set as s_0.

The Taylor expansion of $c_d(s)$ in the neighborhood of s_0 is given as follows. With no loss of generality, let $s_0 = 0$,

$$c_d(s) = c_d(0) + sc'_d(0) + \frac{s^2}{2}c''_d(0) + \frac{s^3}{6}c'''_d(0) + o(s^3) \tag{6}$$

where $c'_d(0) = \frac{dc_d}{ds}|_{s=s_0}$, $c''_d(0) = \frac{d^2c_d}{ds^2}|_{s=s_0}$, $c'''_d(0) = \frac{d^3c_d}{ds^3}|_{s=s_0}$ and $\lim_{s\to 0} o(s^3)/s^3 = 0$. According to Frenet equations[17], we have

$$\begin{aligned} c'_d(0) &= \alpha \\ c''_d(0) &= \kappa\beta \\ c'''_d(0) &= -\kappa^2\alpha + \kappa'\beta + \kappa\tau\gamma \end{aligned} \tag{7}$$

Thus, substitute (7) into (6) and we have

$$c_d(s) = c_d(0) + (s - \frac{\kappa^2}{6}s^3)\alpha + (\frac{\kappa}{2}s^2 + \frac{\kappa'}{6}s^3)\beta + \frac{\kappa\tau}{6}s^3\gamma + o(s^3) \tag{8}$$

In the Frenet frame attached to s_0 , the parametric equations of above curve can be represented as

$$\begin{cases} \mathrm{t}(s) = s - \frac{\kappa^2}{6}s^3 + o(s^3) \\ \mathrm{n}(s) = \frac{\kappa}{2}s^2 + \frac{\kappa'}{6}s^3 + o(s^3) \\ \mathrm{b}(s) = \frac{\kappa\tau}{6}s^3 + o(s^3) \end{cases} \tag{9}$$

This is the local canonical form of the desired $c_d(s)$ at $s_0 = 0$. For any point of the 3-dimension contour discussed in this paper, $\kappa\tau \neq 0$.

C. Local Contouring Error Estimation

To estimate the contouring error locally, there are two methods mainly, one is the tangent line approximation (first-order approximation) and the other the circular approximation. The tangent line approximation is qualified for contouring control of small-curvature contours and suitable for multi-axis motion systems. The circular approximation, utilizes the osculating circle to help estimating the contouring error, improves the contouring error estimation accuracy

compared with tangent line method. However, circular approximation is limited to biaxial system and hard to be applied for multi-axis system. In this paper, a local approximation curve is proposed to estimate the contouring error based on desired contour's canonical form, which has the same curvature, torsion and Frenet frame in the neighborhood of the same point.

Ignoring the high-order infinitesimal parts of above $\mathrm{t}(s)$, $\mathrm{n}(s)$ and $\mathrm{b}(s)$ in the local canonical form (9) of the desired $c_d(s)$, a novel cubic curve

$$\tilde{c}(s) = (s, \frac{\kappa}{2}s^2, \frac{\kappa\tau}{6}s^3)$$

can be used to approximate the desired contour in the neighborhood of $s_0 = 0$. It's easy to verify that $\tilde{c}(s)$ has the same curvature, torsion and Frenet frame with $c_d(s)$ at $s_0 = 0$.

The Taylor expansion (6) can be rewritten as the following by the proposed natural local approximation

$$c_{dh}(s) = c_d(0) + s\alpha + \frac{\kappa}{2}s^2\beta + \frac{\kappa\tau}{6}s^3\gamma \tag{10}$$

While the corresponding expressions by the first-order approximation and the circular approximation are

$$c_{dl}(s) = c_d(0) + s\alpha \tag{11}$$

$$c_{dc}(s) = c_d(0) + \frac{\sin\theta}{\kappa}\alpha + \frac{1-\cos\theta}{\kappa}\beta \tag{12}$$

Obviously, the first-order approximation is not suitable for nonlinear contours ($\kappa \neq 0$). As for the circular approximation, when θ is small enough, $\theta = s\kappa$ and c_{dc} is the same as c_{dh} in the planar case. So the circular approximation can be seen as the second-order approximation but is limited to the planar contours or small torsion spatial ones.

As shown in Fig. 2, the approximation curve's projections can be represented by

$$\mathrm{n} = \frac{\kappa}{2}\mathrm{t}^2 \tag{13}$$

on osculating plane and on rectifying plane it's

$$\mathrm{b} = \frac{\kappa\tau}{6}\mathrm{t}^3 \tag{14}$$

For any point $(\mathrm{t}, \mathrm{n}, \mathrm{b})$ in the neighborhood of $c_d(t)$, We can find the corresponding point $(\mathrm{t}, \frac{\kappa}{2}\mathrm{t}^2, \frac{\kappa\tau}{6}\mathrm{t}^3)$ on the approximation curve to help estimating the contouring error. To realize the decoupling control of contouring error in the task frame, the estimated contouring error along the normal (ε_n) and binormal (ε_b) direction can be defined as

$$\varepsilon_\mathrm{n} = \mathrm{n} - \frac{\kappa}{2}\mathrm{t}^2 \tag{15}$$

$$\varepsilon_\mathrm{b} = \mathrm{b} - \frac{\kappa\tau}{6}\mathrm{t}^3 \tag{16}$$

By above definitions, the estimated contouring error can be presented as

$$\varepsilon_c = \sqrt{{\varepsilon_n}^2 + {\varepsilon_b}^2} \tag{17}$$

In the following, decoupled controller would be designed to assign different dynamics to tangential, normal and binormal direction with an emphasize on minimizing the contouring error (both ε_n and ε_b).

III. Contouring controller design and analysis

In this section, firstly the system dynamics in world Cartesian frame is transformed into Frenet frame. After that, a PD controller is designed to stabilize the error dynamics system obtained by the above estimated contouring errors.

A. System Dynamics in Frenet Frame

The system dynamics of a typical 3-axis control system in the world frame $\mathscr{F}_w$ is shown below

$$M\ddot{w}(t) + B\dot{w}(t) + F(\dot{w}(t)) = Ku(t) \tag{18}$$

where 3×3 diagonal matrixes M, B and K represent equivalent mass, viscous friction coefficient and driver gain respectively. F is the Column friction dependent on velocity $\dot{w}$, and $u(t)$ is the 3×1 control input. For convenience, parameter t is canceled in the following discussion.

At first, the above dynamics in world frame are transformed into the Frenet frame by taking the first and second order derivative to the transformation (3) with respect to time t.

$$\begin{cases} \dot{w} = \dot{R}f + R\dot{f} + \dot{w}_d \\ \ddot{w} = \ddot{R}f + 2\dot{R}\dot{f} + R\ddot{f} + \ddot{w}_d \end{cases} \tag{19}$$

The time derivative of R is

$$\dot{R} = -vRG$$

where $v = \|\dot{w}_d\|$, $G = \begin{bmatrix} 0 & \kappa & 0 \\ -\kappa & 0 & \tau \\ 0 & -\tau & 0 \end{bmatrix}$ and $\ddot{R} = -\frac{d(vRG)}{dt}$.

Thus, we can get the system dynamics in Frenet frame by substituting (19) into (18)

$$M_F\ddot{f} + C_F\dot{f} + K_F f = u_F \tag{20}$$

where

$$\begin{aligned} M_F &= MR, \\ C_F &= 2M\dot{R} + BR, \\ K_F &= M\ddot{R} + B\dot{R}, \\ u_F &= K(u - u_d) - F(\dot{w}), \\ u_d &= K^{-1}(M\ddot{w}_d + B\dot{w}_d) \end{aligned}$$

The feedforward compensation u_d depends on the system dynamics and reference input contour.

B. Decoupled Controller Design

Appropriate error states are chosen to transform the system dynamics in the task frame (20) into error dynamics system and corresponding controller is designed to guarantee its stability.

Taking $z_1 = \mathrm{t}$, $z_2 = \mathrm{n} - \frac{\kappa}{2}\mathrm{t}^2$ and $z_3 = \mathrm{b} - \frac{\kappa\tau}{6}\mathrm{t}^3$ as the control system states, where z_1, z_2 and z_3 represent the tangential error, normal and binormal estimated contouring errors respectively.

Let $Z_1 = [z_1, z_2, z_3]^T$, $Z_2 = \dot{Z}_1$ and

$$f = Z_1 + [0, \frac{\kappa}{2} z_1^2, \frac{\kappa\tau}{6} z_1^3]^T \tag{21}$$

The system dynamics in Frenet frame can be rewritten into the following equation

$$M_Z \dot{Z}_2 + G(Z_1, Z_2) = u_Z \tag{22}$$

where $u_Z = u_F$,

$$M_Z = M_F \begin{bmatrix} 1 & 0 & 0 \\ \kappa z_1 & 1 & 0 \\ \frac{\kappa\tau}{2} z_1^2 & 0 & 1 \end{bmatrix}$$

$$G(Z_1, Z_2) = M_F \begin{bmatrix} 0 \\ \kappa \dot{z}_1^2 \\ \kappa\tau z_1 \dot{z}_1^2 \end{bmatrix} + C_F \begin{bmatrix} \dot{z}_1 \\ \dot{z}_2 + \kappa z_1 \dot{z}_1 \\ \dot{z}_3 + \frac{\kappa\tau}{2} z_1^2 \dot{z}_1 \end{bmatrix} + K_F \begin{bmatrix} z_1 \\ z_2 + \frac{\kappa}{2} z_1^2 \\ z_3 + \frac{\kappa\tau}{6} z_1^3 \end{bmatrix}$$

Considering that the control cycle of real-time applications is at the level of *ms* or even shorter, M_Z is regarded as a constant matrix in each cycle.

The error dynamics system (22) is time-varying and nonlinear. In this paper, a feedback linearization compensation is adopted. The controller u_Z is proposed in the following form

$$u_Z = M_Z V(Z_1, Z_2) + G(Z_1, Z_2) \tag{23}$$

where $G(Z_1, Z_2)$ is computable and has been compensated.

By choosing $V(Z_1, Z_2) = -K_P Z_1 - K_D Z_2$, the PD scheme, where K_P and K_D are all diagonal matrixes, we can transform (22) into state-space form as follows

$$\begin{bmatrix} \dot{Z}_1 \\ \dot{Z}_2 \end{bmatrix} = \begin{bmatrix} 0 & I \\ -K_P & -K_D \end{bmatrix} \begin{bmatrix} Z_1 \\ Z_2 \end{bmatrix} \tag{24}$$

It's easy to prove that the above autonomous system is asymptotically stable if K_P and K_D are positive definite matrixes by Lyapunov's stability theorem [18].

Different control parameters of K_P and K_D are chosen to assign different dynamics to the tangential error and estimated contouring error. The contouring error can be directly decreased by increasing the corresponding parameters.

Thus, the resulted controller in world frame can be expressed as

$$u(t) = K^{-1}(M_Z(t)V(t) + G(t) + F(\dot{w})) + u_d(t) \tag{25}$$

where K is always invertible.

IV. Experiments and discussions

To investigate the performance of the proposed contouring control method based on natural local approximation, compared with first-order approximation based method, simulations of 3-axis system and experiments on a biaxial XY-stage are conducted in this section.

A. Simulation and Discussion

A simple helix curve was chosen as the reference input

$$\begin{cases} x = a\cos(\omega t) \\ y = b\sin(\omega t) \\ z = ct \end{cases} \tag{26}$$

with $a = 0.03m$,$b = 0.01m$, $c = 0.1m$ and $\omega = 2\pi$.

The real axial dynamics of simulated 3-axis control system were $G_x = 1/(s^2 + 200s)$, $G_y = 1/(s^2 + 225s)$ and $G_z = 1/(s^2 + 180s)$. Considering the dynamics parameter uncertainty, the identified viscous friction coefficient matrix $B = diag(205, 230, 180)$ in the controller design. Obviously, the axial dynamics were not matched to each other. Besides, the control cycle is 1 ms.

Referred to [7], the desired error dynamics would be designed in the following form

$$(s^2 + 2\zeta(2\pi f)s + (2\pi f)^2)\varepsilon = 0$$

where f is the bandwidth for some motion direction and ζ is the corresponding damping ratio.

The controller parameter matrix K_P and K_D can be designed as

$$K_P = diag((2\pi f_t)^2, (2\pi f_n)^2, (2\pi f_b)^2)$$

$$K_D = diag(4\pi\zeta_t f_t, 4\pi\zeta_n f_n, 4\pi\zeta_b f_b)$$

To obtain the best transient performance, ζ_t, ζ_n and ζ_b are always set to be one.

In the simulations and following experiments, real contouring error of every actual point was calculated by finding the shortest distance between the actual point with abundant points on the desired contour, which were in the neighborhood of current desired point.

Different dynamics were assigned to the tangential, normal and binormal directions by setting $f_t = 5$,$f_n = 15$,$f_b = 10$. Four periods' data was taken to verify the efficiency of two methods. The mean contouring error obtained by the method based on first-order approximation is 11.46μm while that based on our proposed method is 7.10μm, about 38% had been decreased. The first two periods' contouring errors obtained by two methods were shown in Fig.3.

To improve the contouring performance, f_n and f_b were increased to 20 and 15 respectively. As shown in Fig.4, the new mean contouring error of first-order based method was 11.23μm with little reduction. While, that obtained by the natural local based method was 4.45μm, with 37% improvement compared with the previous.

According to above simulation results, the contouring performance can be improved directly by increasing corresponding control parameters of the natural local approximation based method, compared with the first-order based one.

B. Experimental Setup

To verify the contouring performance of the proposed method for biaxial systems, experiments on a ball-screw drive XY-stage were conducted. Coulomb frictions of the experimental system were $x_+ = 0.12$V, $x_- = 0.11$V, $y_+ = 0.07$V

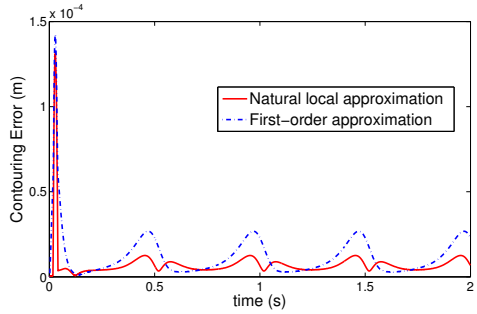

Fig. 3. Contouring errors obtained by two methods with $f_t = 5, f_n = 15, f_b = 10$

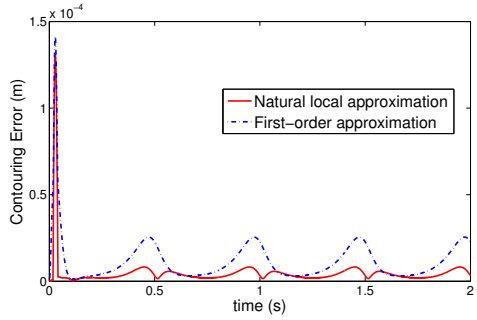

Fig. 4. Contouring errors obtained by two methods with $f_t = 5, f_n = 20, f_b = 15$

and $y_- = 0.06$V. The identified transfer functions of two axes from the input voltage V to the output position m are $16.23/(s^2 + 798.5s)$ and $17.58/(s^2 + 862.75s)$. Obviously, the tracking capabilities of two axes are not matched.

To carry out the proposed method in 2-dimension plane, some detail was needed to pay attention to. For plane curve, the corresponding 2-dimension Frenet frame is a right-hand frame which only depends on the tangent vector. The bending direction of the curve is not always the same with the normal vector. Therefore, a relative curvature is needed to approximate 2-dimension plane contour.

$$\kappa_r = \frac{\dot{x}_d \ddot{y}_d - \dot{y}_d \ddot{x}_d}{\dot{x}_d^2 + \dot{y}_d^2} \tag{27}$$

The reference contours were ellipse (a variable-curvature contour) and Figure-'8' (a sharply variable-curvature contour)

$$\text{Ellipse}: \begin{cases} x = 0.03(1 - \cos(\omega t)) \\ y = 0.01 \sin(\omega t) \end{cases}$$

$$\text{Figure} - 8: \begin{cases} x = 0.03(1 - \cos(\omega t)) \\ y = 0.03 \sin(2\omega t) \end{cases}$$

Under the drivers' saturation ($\pm 10V$), high speed experiments were conducted, where $\omega = 1.8\pi$ ($v_{max} = 10$ m/min) for ellipse and $\omega = \pi$ ($v_{max} = 12$ m/min) for Figure-'8'.

C. Experiments Results

Controller parameter f_n (representing the normal direction) was set as 60, 80 or 100 to strengthen the contouring performance. Meanwhile, f_t (representing the tangential direction) was fixed as 15 to guarantee the tracking performance under drivers' saturation.

The contouring error ε_c, tracking error e and control input of both axes were recorded to compare different methods' performance.

1) Elliptical Case: As recorded in Table.I, the contouring error, obtained by natural local approximation based method, decreased significantly with the increase of control parameter f_n, though the tracking error and control input almost stayed the same. By contrast, the contouring performance of first-order approximation based method was improved only a little. The natural local based method yields much smaller contouring error (RMS, 3.62μm) than the first-order based one (RMS, 13.20μ m) by an improvement of 72.4% at the same control parameter ($f_t = 15, f_n = 100$). Fig.5 illustrates the contouring errors obtained by two methods under $f_t = 15$ and $f_n = 100$.

TABLE I

THE ELLIPSE CONTOUR: $\omega = 1.8\pi$ AND $f_t = 15$

		$\varepsilon_c(\mu$m)		e(mm)		Con. Input(V)	
	f_n	Max	RMS	Max	RMS	U_x	U_y
Natural Local	60	27.77	9.91	2.16	0.66	6.03	2.00
	80	15.07	5.60	2.15	0.66	6.03	2.01
	100	12.21	3.64	2.14	0.65	6.03	2.00
First-order	60	40.07	15.15	2.17	0.66	6.03	2.01
	80	37.28	13.45	2.15	0.65	6.03	2.01
	100	34.17	13.20	2.14	0.65	6.03	2.01

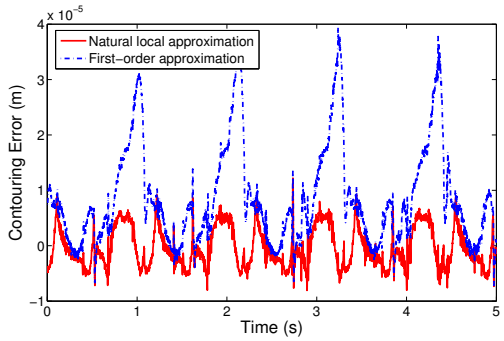

Fig. 5. Ellipse Case : Contouring errors obtained by two methods with $f_t = 15$, $f_n = 100$

2) Figure-'8' Case: Similar results were obtained in the Figure-'8' case. As shown in Table.II, the contouring errors decrease dramatically for natural local based method, while change a little for first-order based one. the smallest contouring error (RMS) of natural local method is 16.69μm with a reduction of 47.6% compared with first-order method, whose smallest value is 31.88μm. Fig.6 illustrates the contouring errors obtained by two methods under the same control parameters ($f_t = 15$ and $f_n = 100$).

V. CONCLUSION

In this paper, a novel contouring control method is proposed for multi-axis control system based on natural local approximation. By studying the local Taylor expansion of

TABLE II

THE FIGURE-'8' CONTOUR: $\omega = \pi$ AND $f_t = 15$

		$\varepsilon_c(\mu\text{m})$		e(mm)		Con. Input(V)	
	f_n	Max	RMS	Max	RMS	U_x	U_y
Natural Local	60	128.29	42.33	4.81	2.14	3.33	6.98
	80	75.23	24.75	4.80	2.13	3.33	6.98
	100	54.22	16.69	4.82	2.13	3.33	6.98
First-order	60	139.61	39.48	4.85	2.16	3.34	6.99
	80	107.97	32.55	4.87	2.16	3.34	6.99
	100	102.16	31.88	4.89	2.18	3.34	7.00

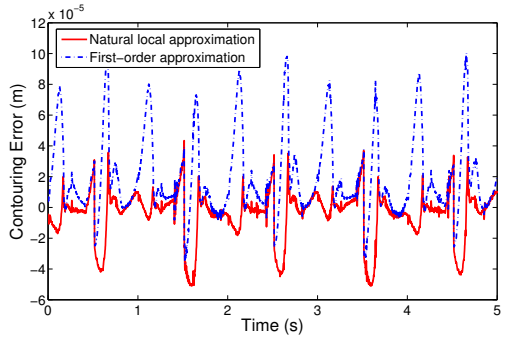

Fig. 6. Figure-'8' Case : Contouring errors obtained by two methods with $f_t = 15$, $f_n = 100$

desired contour, an approximation curve is utilized to help estimating the contouring error. In order to achieve decoupling control of the estimated errors, the system dynamics in the task frame is transformed from the fixed world frame at first. Then, error dynamics is established by replacing the coordinates in task frame with estimated errors. A PD controller is designed in the task frame to assign different dynamics to the tangential error and the estimated contouring error with an emphasize on minimizing the latter one. Simulations of 3-axis control system and experiments on a biaxial XY-stage have verified that the contouring performance can be improved dramatically by our method in high speed and large curvature cases, compared with first-order approximation based method.

REFERENCES

[1] Y. Koren. Cross-coupled biaxial computer control for manufacturing system. *Transactions of ASME, Journal of Dynamic Systems, Measurement and Control*, 102(4):265–272, 1980.

[2] Y. Koren and C.C. Lo. Variable gain cross coupling controller for contouring. *CIRP Proc.-Manufacturing Systems*, 40:371–374, 1991.

[3] S.-S. Yeh and P.-L. Hsu. Estimation of the contouring error vector for the cross-coupled control design. *IEEE/ASME Transactions on Mechatronics*, 7(1):44 –51, Mar 2002.

[4] S.-S. Yeh and P.-L. Hsu. Theory and applications of the robust cross-coupled control design. In *Proceedings of American Control Conference*, pages 791–795, 1997.

[5] G.-J. Wang and T.-J. Lee. Neural-network cross-coupled control system with application on circular tracking of linear motor xy table. In *Neural Networks, 1999. IJCNN'99. International Joint Conference on*, volume 3, pages 2194–2199. IEEE, 1999.

[6] K.L. Barton and A.G. Alleyne. A cross-coupled iterative learning control design for precision motion control.

[7] G.T.-C. Chiu and M. Tomizuka. Contouring control of machine tool feed drive systems: a task coordinate frame approach. *IEEE Transactions on Control Systems Technology*, 9(1):130–138, 2001.

[8] D. Zhang, Y. Lou, and Z. Li. Geometric contouring control on the smooth surface. In *Proceedings of IEEE/RSJ International Conference on Intelligent Robots and Systems*, pages 4496–4501, 2006.

[9] C.-L. Chen and K.-C. Lin. Observer-based contouring controller design of a biaxial stage system subject to friction. *IEEE Transactions on Control Systems Technology*, 16(2):322 –329, March 2008.

[10] C. Hu, B. Yao, and Q. Wang. Coordinated adaptive robust contouring control of an industrial biaxial precision gantry with cogging force compensations. *IEEE Transactions on Industrial Electronics*, 57(5):1746 –1754, May 2010.

[11] Y. Lou, Z. Li, and Y. Zhong. Dynamics and contouringcontrol of a 3-DoF parallel kinematics machine. *Mechatronics*, 21(1):215–226, 2011.

[12] Y. Lou, N. Chen, and Z. Li. Task space based contouring control of parallel machining systems. In *Proceedings of IEEE/RSJ International Conference on Intelligent Robots and Systems*, pages 2047–2052, 2006.

[13] J. Yang and Z. Li. A novel contouring error estimation for position loop-based cross-coupled control. *IEEE/ASME Transactions on Mechatronics*, 16(4):643–655, 2011.

[14] S.-L. Chen and K.-C. Wu. Contouring control of smooth paths for multiaxis motion systems based on equivalent errors. *IEEE Transactions on Control Systems Technology*, 15(6):1151–1158, 2007.

[15] C. Hu, B. Yao, and Q. Wang. Global task coordinate frame-based contouring control of linear-motor-driven biaxial systems with accurate parameter estimations. *IEEE Transactions on Industrial Electronics*, 58(11):5195 –5205, Nov. 2011.

[16] B. Yao, C. Hu, and Q. Wang. An orthogonal global task coordinate frame for contouring control of biaxial systems. *IEEE/ASME Transactions on Mechatronics*, 17(4):622–634426, 2012.

[17] M.D. Do Carmo. *Differential Geometry of Curves and Surfaces*. Prentice-Hall, Inc., Englewood Cliffs, New Jersey, 1976.

[18] H. Khalil. *Nonlinear Systems*. Prentice Hall, 3rd edition, 2002.